Computers, Materials & Continua

Tech Science Press

https://doi.org/10.32604/cmc.2026.080895

ARTICLE

An Intelligent Thermal Monitoring Platform for Manufacturing Workshop Power Distribution Systems

Junyi Wang[1], Jianghai Geng[1,*], Jiaqi Liu[2] and Haibin Zhu[3]

[1]Hebei Provincial Key Laboratory of Power Transmission and Transformation Equipment Security Defense, North China Electric Power University, Baoding, China

[2]State Grid Beijing Chaoyang Electric Power Company, Beijing, China

[3]The Department of Computer Science and Mathematics, Nipissing University, North Bay, ON, Canada

*Corresponding Author: Jianghai Geng. Email: gengjianghai@163.com

Received: 25 February 2026; Accepted: 21 April 2026; Published: 15 June 2026

ABSTRACT: In intelligent manufacturing and remanufacturing systems, the thermal safety of the power distribution infrastructure is crucial for ensuring production continuity, equipment reliability, and operational resilience. Traditional temperature monitoring methods often have problems such as high deployment costs, strong environmental sensitivity, or limited physical interpretability in distributed workshop environments. To address these limitations, this study proposes a physically information-driven intelligent thermal color-changing fault identification framework. Based on thermochromic experiments, irreversible color-changing coatings are selected, which are combined with a visual-based computing pipeline for autonomous overheating detection. The framework proposes a thermal fault temperature identification algorithm based on the self-organizing map (SOM) neural network, which improves the generalization ability through RGB channel normalization; multiple random initialization and optimal screening mechanisms are introduced to explore the global optimal solution in the weight space, addressing the issues of sensitive initial weights and easy falling into local minima; the best matching unit (BMU) identification strategy is used to achieve efficient mapping from the RGB feature space to the physical temperature quantity. This algorithm can effectively convert physical color information into a visual temperature field, providing a new idea for thermal fault monitoring and temperature identification of power distribution lines in manufacturing workshops. To evaluate its engineering applicability, a noise resistance experiment with dual scenarios, dual samples, and five noise levels was designed, quantitatively analyzing the absolute error (AE) and F1 score of the algorithm under different noise levels. Laboratory case studies show that under moderate noise interference ($\sigma < 0.04$), the algorithm still maintains a high recognition accuracy, verifying its robustness and practical potential in complex industrial site environments. This study embeds the physically constrained material response mechanism into the intelligent visual framework, establishing a new paradigm for computer vision-based manufacturing systems.

KEYWORDS: Computer vision-based; manufacturing workshops; power distribution; thermal faults

1 Introduction

The manufacturing workshop serves as the core facility for industrial production, encompassing equipment operation, production processes, power supply and distribution, safety management, and other critical aspects [1]. With diverse electrical equipment and complex load types, the workshop's power supply and distribution system must meet the following requirements: Ensure continuous and stable operation of production equipment; Provide flexible operational and maintenance capabilities, supporting maintenance without power interruption [2]. Therefore, establishing a secure, efficient, and flexible power supply and distribution system for manufacturing workshops is of paramount importance.

The power supply and distribution lines in manufacturing workshops are primarily responsible for safely and reliably delivering electrical energy from substations to various electrical equipment. Common faults in power supply lines include short circuits, overloads, poor contacts, insulation damage, and externally induced failures. Among these, poor contacts and short circuits are the most prevalent hazardous [3]. Special protective measures must be implemented in the lines to prevent power outages, equipment damage, or even fire incidents caused by circuit failures [4].

However, due to the number of power supplies and distribution, the high inspection frequency, and the inherent limitations of infrared temperature measurement methods [5], maintenance personnel often face high workloads and low operational efficiency. Once, overheating faults in power systems could not be detected in time, which are potential risks to the safety of the transmission and distribution line [6–8].

In the inspection and real-time monitoring of thermal faults of power systems, the construction of an efficient temperature sensing system is a critical component [9]. The system could rapidly locate fault positions and accurately identify temperature, and then provide operation and maintenance personnel with sufficient time to handle the fault and take preventive measures [10]. More than a comprehensive acquisition of temperature data during fault occurrences, combined with big data analysis techniques, could support the optimization of power grid design and effectively reduce the incidence of overheating-related faults [11,12]. Based on this, the power system has begun its intelligent transformation. And with the deep integration of industrial Internet of Things technology, smart grids are evolving into sophisticated cyberphysical systems characterized by a tight coupling between physical equipment, sensor networks, and an algorithmic model.

Tong et al. proposed a method based on tensor block-matching, which achieves fault localization by collecting the surface temperature of a distribution cabinet and using complex algorithms to reconstruct the internal three-dimensional temperature field [13]. Although they offer high recognition accuracy, their application is often constrained by the cost of specialized equipment, the real-time requirements of algorithmic computation, and their dependence on the equipment's heat transfer model, posing challenges for universal, low-cost deployment across the numerous and dispersed connections and lines in distribution networks.

Liu et al. proposed a method introducing the PSA module based on YOLOv7 to realize the information interaction between local and global channels and improve the precision recognition of the model for devices of different scales [14]. Jiang et al. proposed a Faster R-CNN-based infrared detection image analysis method for abnormal equipment within substations to realize intelligent identification and cause analysis of faulty equipment in substations [15]. Although high diagnostic accuracy is achieved, these serious cases rely on costly specialized infrared imaging equipment, which greatly increases the cost and influences the flexibility of deployment.

Some researchers consider converting the temperature changes of the equipment into visible color information and use algorithms to identify this temperature based on camera acquisition. Gu et al. developed a monochromatic irreversible thermochromic material that undergoes a permanent color change at 150°C and applied it to detect power grid overheating faults [16]. Based on the physical laws of irreversible thermochromic materials to correlate color changes with surface temperature, these materials can provide visual temperature indication without the need for external power sources or complex sensing devices [17,18]. Wan et al. developed a multistage responsive thermochromic coating by integrating reversible microcapsules and irreversible ammonium metavanadate within a silicone rubber matrix [19]. For the timely detection of abnormal heat, Dong et al. proposed a reversible temperature indication method and used the coating test to identify the thermal defect of a dry hollow reactor [20].

However, existing studies on thermochromic coatings mainly focus on material preparation and performance evaluation, while limited research has systematically integrated such materials into an intelligent manufacturing-oriented identification framework. Most reported applications rely on manual inspection or simple color comparison, lacking autonomous localization, quantitative inversion, and continuous fault evolution tracking capabilities. To bridge this gap, it needs a physics-informed intelligent thermo-chromic fault identification framework.

In terms of thermal monitoring, thermal monitoring in industry has matured in both contact-based and infrared non-contact methods, but significant limitations remain. Contact-based approaches offer pointwise accuracy but suffer from complex power lines and limited spatial coverage. Infrared thermography enables full-field temperature measurement, yet it is costly, sensitive to surface emissivity, and lacks intelligent data analysis capabilities [21]. Recently, vision-based thermal monitoring has been used as a promising alternative: thermochromic materials combined with RGB cameras can achieve high-resolution temperature estimation, but these methods depend on surface modification and are susceptible to illumination, viewing angle. Multimodal image fusion improves visualization by integrating visible and infrared images, yet the underlying temperature computation remains inefficient, restricting real-time deployment on edge devices. Purely visual deep learning methods attempt to infer temperature directly from RGB images, but their generalization and robustness in complex industrial environments are still not good enough. Overall, available research primarily focuses on single-algorithm optimization, lacking a full-stack design from data acquisition to application services. Developing an intelligent, robust, and computationally efficient vision-based thermal monitoring system is still a critical part of industrial IoT.

This study proposes a physics-informed intelligent thermo-chromic fault identification framework tailored for manufacturing and remanufacturing systems. This structured pipeline embeds experimentally established color–temperature models into a computationally efficient vision framework, achieving interpretable and real-time thermal fault recognition suitable for edge deployment in industrial environments. Compared with conventional Computer Vision-based image recognition approaches, the proposed method presents the following advantages: Physics–Data Fusion and Manufacturing-Oriented Robustness.

Therefore, this work contributes to the emerging paradigm of Computer Vision-based in Manufacturing Systems by demonstrating how material intelligence (thermo-chromic coatings) and algorithmic intelligence (vision-based inverse modeling) can be synergistically integrated into a deployable, interpretable monitoring framework.

2 Study of a Multicolor Irreversible Thermo-Chromic Coating

2.1 Materials

The main raw materials used in this study are as follows: cobalt sulfate heptahydrate ($CaSO_4.7H_2O$, analytical grade) supplied by Sinopharm Chemical Reagent Co., Ltd.; manganese sulfate ($MnSO_4$, analytical grade) purchased from Aladdin Reagent (Shanghai) Co., Ltd.; cobalt sulfate ($CoSO_4$, analytical grade) obtained from Sinopharm Chemical Reagent Co., Ltd.; copper sulfate ($CuSO_4$, analytical grade) supplied by Sinopharm Chemical Reagent Co., Ltd.; silicone resin (SiH_4, 50 wt.) provided by Shenzhen Jinbosheng Technology Co., Ltd.; epoxy resin ($C_{21}H_{23}ClFNO_{24}$, 50 wt.) obtained from Jinan Linhai Chemical Co., Ltd.; and xylene (analytical grade) purchased from Sinopharm Chemical Reagent Co., Ltd.

2.2 Experimental Method

The prepared low-and medium-temperature multicolor irreversible thermo-chromic coating was applied onto tinplate substrates at room temperature (25°C) using an adjustable film applicator. The coating thickness was controlled at 30 μm. After complete drying, the coated plates were cut into rectangular specimens with dimensions of 30 mm × 20 mm for subsequent experiments. Thermo-chromic performance tests were conducted in the temperature range of 50°C–200°C with an interval of 10°C. Each sample was individually heated on a heating stage and maintained at the target temperature for 5 min. After heating, the samples were removed and allowed to cool naturally to room temperature. The corresponding color change data were then recorded for further analysis and model construction.

2.3 Multicolor Thermo-Chromic Experiments

Based on the current Classification Standard for Defects of Distribution Network Equipment (Q/GDW 745) and field investigation results, the target operating temperature range was determined to be 50°C–200°C, with a heating duration of 5 min to induce thermally driven color changes corresponding to thermal fault conditions in distribution equipment. The study proposed a low-and medium-temperature multicolor irreversible thermo-chromic coating that enables stable multicolor transitions across the target temperature range.

The primary components of irreversible thermo-chromic coating at low and medium temperatures were determined, as summarized in Table 1. The formulation by mass percentage was: matrix resin:pigment:filler:solvent = 30:40:30:30. The experimental samples were prepared according to this formulation for comparative testing and performance evaluation.

Table 1: Main components of the low- and medium-temperature irreversible thermo-chromic coating.

Sample	Matrix Resin	Thermo-Chromic Pigments	Fillers	Solvent
1	Epoxy resin	Copper sulfate, manganese sulfate	Aluminum oxide, titanium dioxide	Xylene

According to the predefined research objectives, multicolor thermo-chromic tests were conducted on the formulated samples. Based on the experimental results, the sample was subjected to sequential calibration experiments to establish the correspondence between temperature and RGB color values. The thermo-cion results are presented in Fig. 1.

Although the experimental results indicate that the sample exhibits pronounced thermo-chromic behavior, intelligent and digital interpretation requires a quantitative representation of color information. Therefore, the colors of the standard thermo-chromic calibration chart need to be quantified to establish a map relationship between color and temperature, providing a fundamental model for computational interpretation.

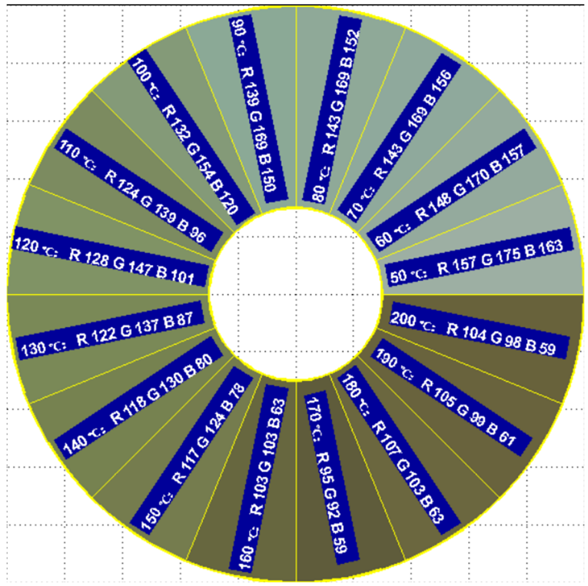

Figure 1: Calibration results of thermo-chromic coating of sample in temperature range of 50°C–200°C.

3 Research on Color Temperature Inversion Model Based on Self-Organizing Map (SOM)

3.1 Dataset Construction and Preprocessing

Based on the RGB value data obtained from the previous color-changing experiments at different temperatures, a standard dataset consisting of 16 discrete temperature points and a temperature range from 50°C to 200°C was constructed, covering the RGB color response of the material under typical working temperatures. To address the potential pixel value fluctuations caused by changes in illumination in practical applications, a strict normalization preprocessing was applied to the original data matrix $X \in \mathbb{R}^{3\times N}$, uniformly mapping the R, G, and B channel values to the 0–1 range. This preprocessing step not only eliminates the dimensional differences among various imaging devices, significantly enhancing the generalization ability of the model, but also lays the foundation for data consistency for its subsequent application in complex environments.

3.2 Robustness Training Strategy for SOM Model

To ensure the stability of the model in actual engineering applications, a Self-Organizing Map (SOM) neural network is employed for unsupervised learning. Meanwhile, since the traditional SOM algorithm is sensitive to the initial weights and is prone to randomness, it may lead to inconsistent prediction results. Therefore, an innovative approach of introducing multiple random initializations and an optimal screening mechanism has been adopted to optimize the SOM algorithm.

Firstly, iterative training is conducted on a 1×16 one-dimensional neuron array; Secondly, 20 independent random inputs and training are set up to explore the global optimal solution of the weight space. This approach effectively overcomes the risk of local minima that may occur in a single training process, ensuring the prediction accuracy and repeatability of the final deployed model, and meeting the standards for industrial-level applications.

3.3 Temperature Inversion Algorithm Based on Topological Mapping

In order to establish an efficient mapping from the RGB feature space to the physical quantity of temperature, after the training is completed, each neuron node is assigned a unique feature temperature label. In practical prediction applications, this model demonstrates extremely high computational efficiency and practicality:

(1) Data consistency preservation: By using the normalized parameters saved during the training stage, the input arbitrary RGB samples are standardized to ensure that the input data is in the same distribution space as the training data.

(2) Best Matching Unit (BMU) identification: By calculating the Euclidean distance between the input sample and the neuron weight matrix, the best matching unit is quickly located.

(3) Temperature inversion: Directly outputs the preset temperature value corresponding to the BMU. This algorithm does not require a complex iterative optimization process, has low computational complexity, and is highly suitable for embedded systems or real-time image processing scenarios. It can quickly and accurately convert the collected color information into a visualized temperature field distribution and has significant engineering application value.

3.4 Results and Discussion

3.4.1 Convergence Analysis of SOM Model Training

Fig. 2a presents the convergence curve of the training error for the SOM model based on the multiple random initialization strategy. During 20 independent training iterations, the average absolute error (MAE) of the model exhibited significant fluctuations. In the initial stage, the error was relatively high (with a maximum value of approximately 4.4°C), which verified the sensitivity of the SOM algorithm to the initial weights and its tendency to get trapped in local optima. However, through the strategy of multiple random initialization and selecting the optimal solution, the model eventually converged to a very low error level. As marked by the red asterisk in the figure, the optimal model was obtained in the 16th training iteration, with its validation set MAE as low as 0.625°C. This result indicates that the proposed multiple initialization strategy effectively avoids the trap of local minima, significantly improving the prediction accuracy and robustness of the model.

3.4.2 Convergence Analysis of SOM Model Training

Fig. 2b shows the mapping relationship between the neuron indices in the optimal SOM model and the corresponding temperatures. The *x*-axis represents the 16 one-dimensional neuron indices, and the *y*-axis represents the temperature value that the neuron represents in the training data. It can be seen that although there is an overall trend of increasing temperature as the index increases, there are non-monotonic fluctuations in specific areas (such as around the neuron indices 5 to 7).

This non-linear mapping reflects the distribution density of training samples in the color space. According to the topological preservation property of SOM, the regions with higher sample density in the training data (i.e., the temperature intervals with significant color changes) will occupy more neuron nodes, thereby causing local stretching or compression of the mapping curve. For example, the curve shows relatively smooth monotonicity in the low-temperature region (approximately 50°C–100°C) and the high-temperature region (approximately 150°C–200°C), while it exhibits larger fluctuations in the medium-temperature region, which may correspond to the temperature segments with larger color change rates or more complex sample distributions in the experimental data. This mapping relationship successfully embedded the discrete temperature labels into the continuous neural array, laying the foundation for subsequent temperature predictions.

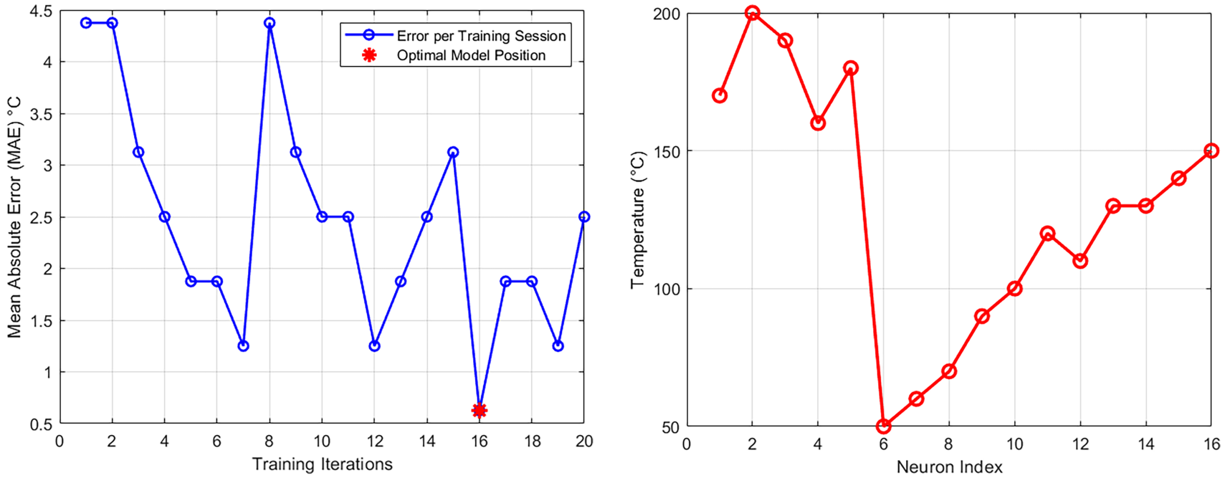

(a) SOM Training Error Convergence Curve (Optimal MAE = 0.625°C)

(b) Analysis of Neuron Temperature Mapping Relationship

Figure 2: SOM training result.

3.4.3 Evaluation of Prediction Performance of SOM Model

The SOM model training is completed on a microcomputer with hardware configuration of Intel Core i5-10500 CPU (3.10 GHz) and 8 GB RAM. Under this configuration, the running time for a single training session is approximately 60 s. Based on the above results, the color temperature inversion model based on SOM achieved extremely high fitting accuracy (MAE < 1°C) at 16 discrete temperature points. This indicates that the model is capable of effectively capturing the nonlinear mapping relationship between the RGB color space and temperature. Compared with traditional polynomial fitting or linear regression methods, the SOM model automatically learns data features through a data-driven approach without complex function forms. Therefore, it has stronger adaptability when dealing with complex physical and chemical responses such as thermochromic materials. The successful construction of this model provides a reliable theoretical basis and algorithmic support for subsequent non-contact temperature field measurements based on images.

4 Intelligent Overheating Fault Identification Method for Manufacturing Systems

4.1 Construction of a Computer Vision-Based Thermal Fault Identification Framework for the Power Supply and Distribution System in the Manufacturing Workshop

The power supply and distribution system in manufacturing workshops, as an important part of industrial digital transformation, its safe and stable operation directly affects the continuous production status of the manufacturing workshop. However, in the complex environment of the manufacturing workshop, which is characterized by high temperature, high humidity, dust, and mechanical vibration, traditional detection methods relying on manual inspection or infrared temperature measurement technology have limitations such as poor real-time performance, high economic cost, and significant sensitivity to the environment. Thus, these methods are unable to meet the requirements of industrial digital transformation. Therefore, it is necessary to establish a Computer Vision-based hot fault identification framework specifically for manufacturing scenarios, in order to achieve intelligent detection and quantitative analysis of thermal faults in the power supply and distribution lines of manufacturing workshops. Therefore, this paper proposes an intelligent identification architecture for thermal faults in the power supply and distribution lines of the manufacturing workshop, which combines the material perception mechanism with Computer Vision-based algorithms. The irreversible thermochromic paint, as the response carrier for thermal faults, is utilized to achieve the physical visualization expression of the thermal faults through the color changes caused by abnormal temperature variations in the power supply and distribution lines. By collecting image data of the line through the camera, the color change information is quantified into computable RGB feature vectors, thereby establishing a mapping process from the physical thermal fault response to digital signals.

To obtain the quantitative relationship between color feature vectors and temperature physical quantities, a data-driven chromaticity-temperature model was established, achieving a one-to-one correspondence between RGB color parameters and physical temperature variables. By applying a computer vision-based difference recognition algorithm and a SOM color temperature inversion method, the intelligent positioning and temperature identification of local thermal anomalies on the line were achieved. This framework has established a technical system where material perception, data modeling, and intelligent recognition operate in synergy, transforming the line thermal fault detection from an inefficient, labor-intensive, and costly manual process to an intelligent decision-making model based on data analysis and algorithm reasoning.

This Computer Vision-based recognition architecture not only realizes the visual representation of physical thermal faults but also possesses the ability for quantitative analysis based on algorithm models, and can monitor and intelligently evaluate the operating status of the power supply and distribution system in real time. This technical system provides technical support for the intelligent operation and maintenance of the power supply system in the manufacturing workshop, and offers a systematic solution for the application of intelligent monitoring technology based on material response in the manufacturing system. The system architecture figure illustrating the entire data flow is shown in Fig. 3.

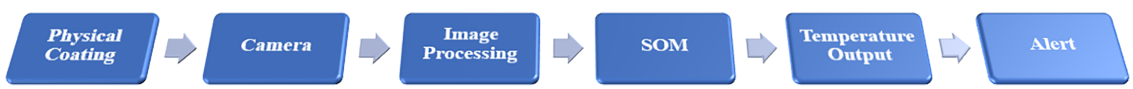

Figure 3: Data flow diagram of system.

4.2 Difficulty Analysis for Intelligent Image Recognition in Complex Environments

The manufacturing workshop, due to its role in industrial production, often has a very complex working environment. Factors such as changes in lighting and dust interference may all affect the quality of video image acquisition, thereby causing a significant reduction in the stability and recognition accuracy of intelligent recognition algorithms. Therefore, developing a visual recognition mechanism with good stability, high recognition accuracy, and strong robustness is the key to achieving intelligent identification of line thermal faults.

In the process, the quality of images captured by the camera is particularly crucial. During the image capture process by a camera, even though the camera itself remains stationary, the images are still subject to two primary sources of interference. The first is Gaussian noise, which is randomly introduced into the image when the camera is operating in low-light conditions or for extended periods. The second is aliasing artifacts (i.e., image distortion) caused by high-frequency details in the scene (such as dense railings or fast-moving objects). These details result in "jagged" or distorted patterns when captured at fixed time intervals. Both of these noise patterns are classified as Gaussian noise. The mitigation of Gaussian noise is conventionally addressed through spatial domain methodologies [22]. Therefore, the study proposes a physical information-driven intelligent identification method for thermal faults based on the SOM color temperature inversion model mentioned earlier, and conducts noise resistance tests against Gaussian noise.

4.3 Intelligent Identification and Robustness Analysis of Line Thermal Failures Based on SOM Color Temperature Model

4.3.1 Experimental Data and Preprocessing

Extract the images taken at two adjacent moments for algorithm verification, namely the reference image (I_{ref}) and the test image (I_{test}). To ensure the robustness of the algorithm, the consistency of image sizes is first checked. If the image sizes do not match, the test image is resampled using the bilinear interpolation method (Bilinear Interpolation) to make it completely aligned with the size of the reference image. After the image data is normalized, the pixel value range is mapped to the interval [0, 1], eliminating the interference of illumination intensity differences on the subsequent analysis.

4.3.2 Detection of Changed Areas

To accurately determine the temperature of the thermochromic regions in the image, a color difference-based segmentation algorithm is employed. Firstly, the Euclidean distance between the test image and the reference image in the RGB color space is calculated to generate the difference map D:

$$D(x,y) = \sqrt{\sum_{c\in\{R,G,B\}} \left(I^{c}_{\text{test}}(x,y) - I^{c}_{\text{ref}}(x,y)\right)^2} \tag{1}$$

Secondly, the global threshold is automatically determined using Otsu's Method, and the difference image is binarized to obtain the initial change mask M_{init}. Then, to eliminate isolated noise points and smooth the regional boundaries, a morphological opening-closing operation with a circular structure element of radius 2 is applied to the mask for post-processing:

$$M_{\text{proc}} = \text{Opening}\big(\text{Closing}(M_{\text{init}}, \text{SE}), \text{SE}\big) \tag{2}$$

4.3.3 Temperature Recognition Model

Since the aforementioned SOM color temperature recognition model has established a nonlinear mapping relationship between the RGB color space and the temperature value during the training stage, temperature can be determined based on this model. First, the pixel point set P of the test image is extracted from the change region mask M_{proc}:

$$P = \{(x,y) \mid M_{\text{proc}}(x,y) = 1\} \tag{3}$$

Subsequently, calculate the average RGB value $(\bar{R}, \bar{G}, \bar{B})$ of the pixels within this area. To meet the input requirements of the SOM model, the normalized RGB values are converted to integer format within the range of [0, 255]. Finally, the temperature value T_{pred} of this area is identified through the trained SOM model:

$$T_{\text{pred}} = f_{\text{SOM}}(\bar{R}, \bar{G}, \bar{B}) \tag{4}$$

where f_{som} represents the identification function of the SOM model.

4.3.4 Noise Robustness Analysis

In order to verify the stability of the proposed SOM color temperature recognition algorithm in complex environments, this test was designed with two scenarios, two samples, and five noise levels. Specifically as follows: Based on the characteristics of the power supply and distribution lines in the intelligent manufacturing workshop, two scenarios are set: the line T-junction and the internal part of the distribution box; for each scenario, two samples of thermochromic images with different temperatures (the T-junction is set at 100°C and 120°C, and the internal part of the distribution box is set at 60°C and 100°C) are provided; Gaussian white noise $\mathcal{N}(0, \sigma^2)$ is introduced, and five levels of noise are set, with standard deviations σ set to 0, 0.01, 0.02, 0.05, and 0.1. For each noise level, the change area detection and temperature recognition process is repeated, and the absolute error (Absolute Error, AE) reflecting the regression accuracy and the F1 value (F1 Score) reflecting the segmentation accuracy of fault distinction segmentation are recorded:

4.3.5 Analysis of Test Results

By comparing the AE and F1 values under different noise levels, the system analyzes the mechanism by which noise affects the performance of the algorithm. A set of representative numerical results was simulated. These data illustrate the trend of the algorithm's performance decline as the noise increases.

(1) Line T-Junction Scenario

Fig. 4 is the diagram of test identification and positioning results. The thermal fault temperature is set at 100°C and 120°C; Fig. 5 shows the color changing before and after.

Figure 4: Diagram of test identification and positioning results of T-junction.

Figure 5: Chart of color changing before and after.

As shown in Figs. 6 and 7, the influence of noise intensity on system performance exhibits a clear dual threshold effect. In terms of temperature inversion, when the noise standard deviation σ is less than 0.04, the mean absolute errors in the 100°C and 120°C scenarios are 0.12°C and 0.15°C, respectively. The analysis of variance shows that there is no significant difference between the groups ($F_{(1,8)} = 1.23$, $p > 0.05$), indicating that the algorithm has high stability in a low-noise environment; however, when σ is greater than 0.04, the error increases rapidly and remains unchanged. The error in the 100°C scenario is 50.2°C, and that in the 120°C scenario is 70.5°C. The analysis of variance shows that there is a significant difference between the groups ($F_{(1,8)} = 48.73$, $p < 0.001$), indicating that the algorithm's performance fails fundamentally in a high-noise environment. In terms of image segmentation, the F1 score shows a non-linear decay with the increase of σ. It drops sharply at $\sigma = 0.04$. The F1 scores in the 100°C and 120°C scenarios drop sharply from a high-precision level close to 1.0 to 0.02, and remain stable at higher noise intensities. Pearson correlation analysis shows that the error in temperature inversion and the F1 score are significantly negatively correlated in the

$\sigma > 0.04$ range ($r = -0.98,\ p < 0.001$), indicating a strong correlation between error saturation and segmentation failure in high noise. Additionally, the differences in error saturation values in different temperature scenarios may be related to the differences in the algorithm's sensitivity to different temperature gradients. These results provide key empirical evidence for the design of algorithm robustness in complex noise environments, suggesting that subsequent research should focus on the decisive influence of the noise threshold $\sigma = 0.04$ (which corresponds to a Power Signal to Noise Ratio (PSNR) of about 28 dB) on system performance.

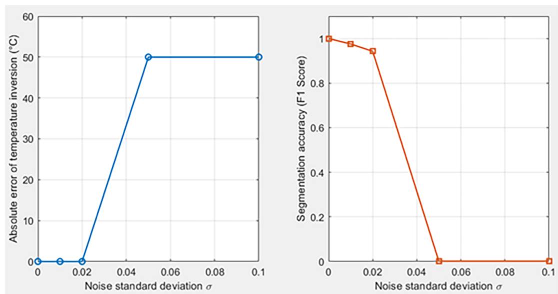

Figure 6: Inversion identification test results at 100°C temperature.

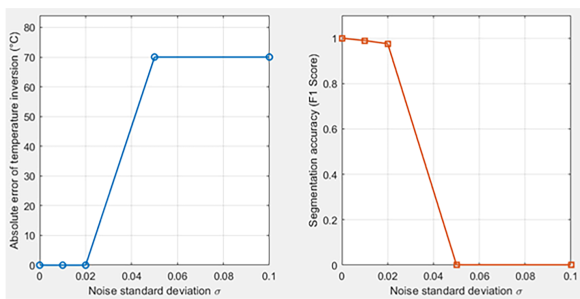

Figure 7: Inversion identification test results at 120°C temperature.

(2) Inside the Distribution Box scenario

Fig. 8 is the diagram of test identification and positioning results. The thermal fault temperature is set at 60°C and 100°C; Fig. 9 shows the color changing before and after.

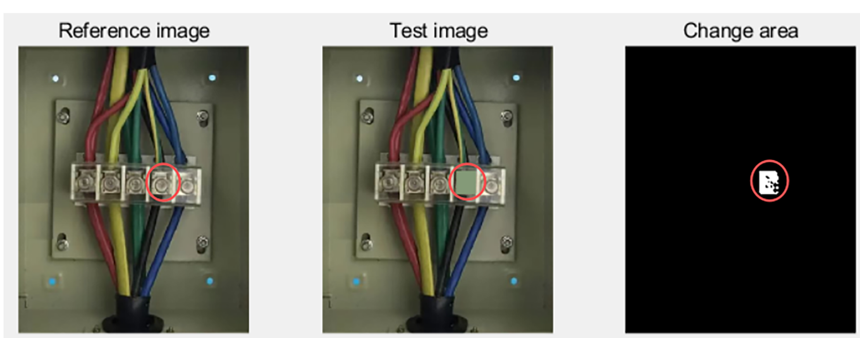

Figure 8: Diagram of test identification and location results in the distribution box.

(a) Unchanged in distribution box (b) 60°C color change (c) 100°C color change

Figure 9: Chart of color changing before and after.

As shown in Figs. 10 and 11, the algorithm performance exhibits a strong nonlinear dependence on the change of the noise standard deviation σ. In the temperature inversion task, when σ increases from 0 to 0.04, the absolute error remains at 0°C; however, when $\sigma > 0.04$, the error immediately undergoes a sudden increase and remains constant (110°C in the 60°C scenario and 70°C in the 100°C scenario), indicating that the algorithm completely loses its temperature identification ability above this threshold. In the segmentation task, the trend of the F1 score with respect to σ is highly consistent with the temperature inversion error: when $\sigma < 0.04$, the F1 score is close to 1.0, demonstrating excellent segmentation performance; when σ exceeds 0.04, the F1 score drops sharply to nearly 0 and remains unchanged, indicating that the algorithm completely fails in target area localization. The Pearson correlation analysis shows that the temperature inversion error and the segmentation accuracy exhibit a significant negative correlation in the $\sigma > 0.04$ range ($r = -0.98$, $p < 0.01$), further confirming the intrinsic correlation between the performance collapse of the two tasks under noise interference. These results collectively indicate the fundamental limitations of the algorithm in its anti-noise performance, namely, there is a clear failure threshold ($\sigma \approx 0.04$), for which the corresponding PSNR is about 28 dB. It provides a crucial empirical basis for subsequent improvements in the algorithm's robustness.

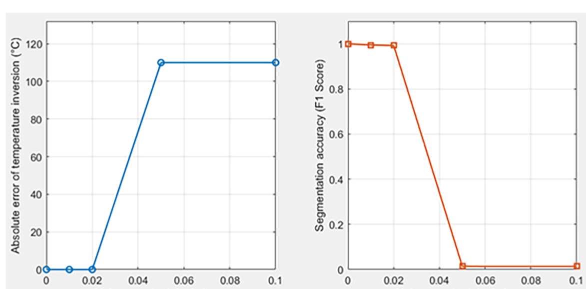

Figure 10: Inversion identification test results at 60°C temperature.

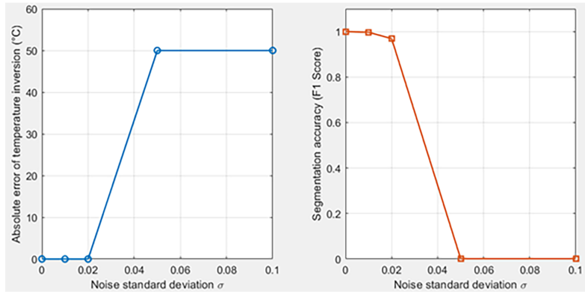

Figure 11: Inversion identification test results at 100°C temperature.

4.4 Limitations

The intelligent identification method for line thermal faults proposed in this paper possesses the basic functions of real-time monitoring and retrieving fault history, and is applicable to remote or enclosed facilities with long inspection cycles. For a large number of line nodes with low individual value, the method utilizes the visible light imaging scheme, which is conducive to achieving an economically feasible universal deployment. Through two scenarios, two samples, and five levels of noise resistance tests of the basic application simulation, the method preliminarily explores the response characteristics and robustness performance under different environmental interference conditions. This method is not merely a simple improvement of the existing temperature measurement technology; rather, it represents a new paradigm of fault diagnosis that integrates physical-chemical changes and visual recognition. Nevertheless, this method still has the following limitations:

(1) The development of a coating is a closed-loop process of "design–preparation–testing–optimization". Currently, this paper is at the basic laboratory research stage. We adopt a modular design approach and prepare samples using laboratory standard methods, then select the formulation ratio with the best comprehensive performance. In the current experimental design, we have not yet deeply covered the standardization of the board manufacturing process, construction performance, paint film performance under complex environments, and the verifiability of the reproducibility of the formulation in industrial production.

(2) Currently, this research has established the framework and completed the basic functional tests, proving that this framework technology is feasible and the logical chain is complete. But the power supply and distribution system in the intelligent manufacturing workshop exhibits a high degree of heterogeneity and scene-dependency, and the deployment and implementation difficulty, technical adaptation requirements, and corresponding resource investment have high uncertainty, which are difficult to be quantified in terms of total cost of ownership (TCO) at the current stage. Therefore, no research has been conducted on deployment and implementation plans, including working conditions, technical requirements, and process requirements, especially in terms of the impact of minor camera vibration, moving objects in the background, or lighting changes over time.

5 Conclusions

This paper focuses on the thermal safety monitoring requirements of power supply and distribution lines in the complex operating environment of intelligent manufacturing workshops, and has constructed a system-level intelligent thermal fault identification platform that integrates material sensing mechanisms and Computer Vision-based algorithms. By integrating irreversible multicolor thermochromic materials with machine vision recognition technology, data-driven color-temperature modeling methods, and numerical inversion algorithms, the automatic location and temperature quantitative identification of thermal faults in the power distribution lines of the manufacturing system have been achieved. This research not only accomplished the optimization of material properties and model construction, but also realized the design of an intelligent monitoring architecture for manufacturing systems, providing a new technical path for low-cost online thermal safety monitoring in industrial scenarios. The main conclusions are as follows.

(1) A multi-color irreversible thermo-chromic coating operating within the temperature range of 50°C to 200°C was successfully formulated. With a mass ratio of resin:pigment:filler:solvent = 30:40:30:30, the coating exhibited stable and distinguishable irreversible color transitions after 5 min of heating within the target temperature range. It provides a reliable physical foundation for constructing a visual temperature-sensing mechanism.

(2) Based on the physical thermochromic experiment data, a color-temperature inversion model based on a self-organizing map (SOM) neural network was successfully built. By adding multiple random initialisations and an optimal selection mechanism, it has addressed the issue of sensitivity to initial weights and ease of getting stuck in a local minimum for traditional algorithms; the stability and generalisation performance of the model were clearly enhanced. The model had achieved a highly efficient and low-complexity mapping from the RGB feature Space to physical temperature Values, and it offered a theoretical Foundation and Algorithm support for subsequent image-based non-contact temperature field measurement.

(3) The intelligent identification method for thermal faults of power supply and distribution lines in a smart manufacturing workshop, which was proposed based on the SOM color-temperature inversion model, realized a closed-loop automatic processing mechanism of "physical sensing-visual recognition-data inversion-intelligent decision-making." The experimental results showed that the recognition algorithm based on the SOM color-temperature model had stable performance at a moderate noise level ($\sigma < 0.04$). Within this range of noise, whether it is a line tee joint or an internal scenario of a distribution box, the algorithm can effectively suppress noise interference; The absolute error (AE) of temperature inversion has been kept at a relatively low level; And maintained a high F1 score, which verified the robustness of this model in a complex industrial field environment.

6 Outlook

As the intelligent manufacturing and remanufacturing systems continue to evolve towards a more digital, networked, and intelligent direction, the operation and safety management of the power supply and distribution systems in manufacturing workshops is gradually shifting from the manual inspection mode to a data-driven intelligent monitoring mode. The proposed thermal fault identification method in this paper, which integrates irreversible multicolor thermochromic materials with Computer Vision-based algorithms, constructs a system monitoring framework that combines material response, visual recognition, and data inversion. Future research will further delve into areas such as material performance optimization, intelligent upgrade of algorithms, and system platform integration, in order to enhance its engineering adaptability and large-scale application potential in manufacturing and remanufacturing systems.

First, at the material level, future research will focus on enhancing the long-term stability and environmental adaptability of the thermochromic coating in complex industrial environments. The complex environmental variables in the manufacturing workshop may have an impact on the color response accuracy and long-term reliability of the coating. Therefore, it is necessary to conduct weather resistance tests and accelerated aging experiments, and the preparation process of the coating, paint film performance testing, construction, packaging process, etc., and based on this, propose the maintenance workflow.

Second, at the algorithm and model level, the color-temperature mapping model will further evolve towards a data-driven intelligent model. The current SOM color temperature inversion model is mainly based on offline training; there are still shortcomings in the robustness of algorithms in complex environments. In the future, more intelligent AI algorithms will be introduced to adaptively compensate to enhance the robustness of the model in the actual manufacturing environment. Some facts will be discussed, such as illumination color temperature, white balance, camera sensor response, and coating aging/soiling. An intelligent recognition model with generalization ability can be established, enabling the system to maintain stable recognition accuracy even under complex conditions.

Third, pilot studies or on-site application verification are carried out, that is, to physically set up a pilot test bench or simulate the power supply environment of an intelligent manufacturing workshop, and to give careful consideration to the complex environment of the intelligent manufacturing workshop, the characteristics of thermal faults, and the thermal anomaly collection equipment. The theory and methods in the laboratory are tested in a real or highly simulated industrial environment, and a systematic quantitative comparison in terms of technology and cost is made with the current related methods.

At the system architecture level, by integrating image recognition and temperature inversion algorithms into edge computing devices, real-time processing and rapid response at the site level could be achieved. Also, some issues will be treated as the main research content and further explored in the subsequent stages, such as frames per second processed on a standard or embedded computer.

Furthermore, it is necessary to combine the normal operating temperature ranges of different devices with the heat resistance characteristics of materials to develop multi-temperature segmented response-type irreversible temperature-indicating coatings. By establishing a hierarchical temperature zone database and implementing intelligent identification strategies, a hierarchical early warning mechanism for different risk levels of thermal faults can be achieved.

Overall, future research will continue to advance along four directions: "improvement of material performance–upgrade of intelligent algorithms–integration of system platforms–expansion of multi-scenario applications", gradually building a system-level artificial intelligence thermal safety monitoring platform covering manufacturing and remanufacturing systems. This platform is expected to achieve a transformation from local heat anomaly detection to intelligent management of the entire power operation status, providing a more comprehensive and sustainable solution for the safe operation and maintenance of power distribution systems in the intelligent manufacturing environment.

Acknowledgement: Not applicable.

Funding Statement: The authors received no specific funding for this study.

Author Contributions: Conceptualization, Junyi Wang, Jianghai Geng, Jiaqi Liu and Haibin Zhu; methodology, Junyi Wang; validation, Junyi Wang, Jianghai Geng and Jiaqi Liu; formal analysis, Junyi Wang, Jianghai Geng and Haibin Zhu; investigation, Jiaqi Liu; resources, Junyi Wang and Jianghai Geng; data curation, Junyi Wang; writing—original draft preparation, Junyi Wang, Jianghai Geng, Jiaqi Liu and Haibin Zhu. All authors reviewed and approved the final version of the manuscript.

Availability of Data and Materials: All data generated or analyzed during this study are included in this article and are available from the corresponding author upon reasonable request.

Ethics Approval: Not applicable.

Conflicts of Interest: The authors declare no conflicts of interest.

References

1. Cai H, Wan J, Chen B. Digital twin-driven multi-factor production capacity prediction for discrete manufacturing workshop. Appl Sci. 2024;14(7):3119. doi:10.3390/app14073119.
2. Hamdeen I, Badran EA, Kotb MF, Elgamal M. Self-healing multi-agent techniques in electric power distribution systems: a review. Renew Sustain Energy Rev. 2025;224(12):116132. doi:10.1016/j.rser.2025.116132.
3. Li C, Yang Z, Yao W, Zou K, Liu H, Lin J, et al. Experimental study of ignition process caused by poor electrical contact of connecter. Process Saf Environ Protect. 2024;189:1517–26. doi:10.1016/j.psep.2024.07.006.
4. Zhang J, Wang J, Li H, Zhang Q, He X, Meng C, et al. A review of reliability assessment and lifetime prediction methods for electrical machine insulation under thermal aging. Energies. 2025;18(3):576. doi:10.3390/en18030576.
5. Balakrishnan GK, Yaw CT, Koh SP, Abedin T, Raj AA, Tiong SK, et al. A review of infrared thermography for condition-based monitoring in electrical energy: applications and recommendations. Energies. 2022;15(16):6000. doi:10.3390/en15166000.
6. Persiani CAF, Sallazar FM, Inoue RS, Valdir Grassi I Jr, Terra MH, Oleskovicz M. Drone-based fault recognition in power systems: a systematic review of intelligent methods. Discov Appl Sci. 2025;7(5):475. doi:10.1007/s42452-025-06774-z.
7. Zhang G, Du Z, Zhang Y, Chen J, Zhang X. Real-time performance evaluation and optimization of electrical substation equipment inspection algorithm based on distributed computing. Int J Low Carbon Technol. 2024;19:1878–87. doi:10.1093/ijlct/ctae136.
8. Faisal MAA, Mecheter I, Qiblawey Y, Fernandez JH, Chowdhury MEH, Kiranyaz S. Deep learning in automated power line inspection: a review. Appl Energy. 2025;385(7):125507. doi:10.1016/j.apenergy.2025.125507.
9. Oukaira A, Hassan A, Ali M, Savaria Y, Lakhssassi A. Towards real-time monitoring of thermal peaks in systems-on-chip (SoC). Sensors. 2022;22(15):5904. doi:10.3390/s22155904.
10. Tang Z, Jian X. Thermal fault diagnosis of complex electrical equipment based on infrared image recognition. Sci Rep. 2024;14(1):5547. doi:10.1038/s41598-024-56142-x.
11. Swain A, Abdellatif E, Mousa A, Pong PWT. Sensor technologies for transmission and distribution systems: a review of the latest developments. Energies. 2022;15(19):7339. doi:10.3390/en15197339.
12. Chuang X, Li L, Zhu L, Wei M, Qiu Y, Xin Y. The design of a real-time monitoring and intelligent optimization data analysis framework for power plant production systems by 5G networks. Energy Inform. 2025;8(1):29. doi:10.1186/s42162-025-00487-8.
13. Tong J, Tan Y, Zhang Z, Zhang Q, Mo W, Zhang Y, et al. Non-intrusive temperature rise fault-identification of distribution cabinet based on tensor block-matching. Global Energy Interconnect. 2023;6(3):324–33.
14. Liu X, Li W, Ji J, Shi G. Infrared image recognition of substation equipments based on improved YOLOv7. Infrar Technol. 2023;47(1):63–71.
15. Jiang J, Liu N, Sun C. Infrared detection method based on faster R-CNN image processing for abnormal equipment in substation. J Shenyang Univ Technol. 2024;46(2):157–64.
16. Gu SQ, Wang HT, Yan BW, Gong H, Li T, Fang SB, et al. Diagnosis of overheating faults in transmission line fittings based on thermochromic coatings. Water Res Pow. 2017;35(11):186–9. doi:10.20040/j.cnki.1000-7709.2017.11.046.
17. Wang S, Xu Z, Chen F, Li S, Bo K, Guo H, et al. Continuously irreversible thermochromic pigments: A-site mismatch driven color-evolution in $La_{1-x}Lu_xCrO_3$ (x = 0, 0.1, 0.2). Ceram Int. 2025;51(6):7243–51. doi:10.1016/j.ceramint.2024.12.159.
18. Xue D, Lv CC, Bi X, Wang Y, Chen Z, Zhao T, et al. Colorful thermochromic microcapsules for visual temperature sensing and moisture-thermal management. Polymer. 2026;344(14):129534. doi:10.1016/j.polymer.2025.129534.
19. Wan X, Xia X, Li C, Yu Z, Yang J, Zhu X, et al. Multistage responsive thermochromic coatings for real-time overheat monitoring and high-temperature accident traceability. Mater Lett. 2026;405:139676. doi:10.1016/j.matlet.2025.139676.
20. Dong B, Wu B, Meng Y. Preparation of reversible thermochromic coatings for dry hollow reactors with thermal defects and the physicochemical properties of discoloration. High Voltage Eng. 2024;50(1):322–30. doi:10.13336/j.1003-6520.hve.20221774.

21. Vollmer M, Möllmann K. Infrared thermal imaging: fundamentals, research and applications. 3rd ed. Berlin/Heidelberg, Germany: Springer; 2018. doi:10.1002/9783527693306.
22. Rani A, Bhogal RK. Efficient real-world image denoising using multi-scale gaussian pyramids. Sci Rep. 2025;15(1):40086. doi:10.1038/s41598-025-23942-8.